A Recursive Algorithm for Joint Time-Frequency Wideband Spectrum Sensing

Joseph M. Bruno and Brian L. Mark
Dept. of Electrical and Computer Engineering
George Mason University, MS 1G5
4400 University Drive, Fairfax, VA
email: jbruno2@gmu.edu; bmark@gmu.edu

***Abstract*—In wideband spectrum sensing, secondary or unlicensed users take signal measurements over a given wide spectrum band and attempt to determine subbands for which the spectrum is idle and thus available for use. Some recent approaches to finding such spectrum holes generally employ some form of edge detection or energy detection. We propose an algorithm for joint time-frequency wideband spectrum sensing based on applying a form of temporal spectrum sensing together with a recursive tree search. The algorithm is able to detect spectrum holes accurately even in the presence of bursting primary signals and primary signals whose power spectral densities have smooth band edges. Numerical results are presented which show the performance gain of the proposed algorithm over earlier approaches to wideband spectrum sensing.**[1]

***Index Terms*—Cognitive radio, spectrum sensing, dynamic spectrum access**

I. Introduction

Due to the rapidly increasing demand for capacity in wireless networks, radio frequency (RF) spectrum access becomes more precious every day. However, it has been shown that fixed frequency allocations have left large portions of the RF spectrum underutilized [1]. Cognitive radio (CR) aims to increase utilization of those bands without disruption to the licensed user [2]. In order to maximize capacity and minimize service disruptions to the primary user (PU), a cognitive secondary user (SU) must employ sophisticated sensing techniques. Spectrum sensing techniques can be organized into three basic categories [3]:

1) *Narrowband:* A single channel is clearly defined, and the SU will only sense that channel.
2) *Multiband:* Multiple narrowband channels, assumed to be independent, have been defined, and the SU must sense each channel. Multiband techniques are useful for applications such as TV whitespace where many channels are clearly defined.
3) *Wideband:* The SU must sense over a wide bandwidth which may contain multiple narrowband channels with unknown boundaries.

Of the three classes, narrowband techniques have been studied most extensively. Well-known detection algorithms for narrowband sensing include energy detection, cyclostationary feature detection, and matched filter detection [4]. Research has also been performed on narrowband sensing algorithms which use hidden Markov models (HMMs) and related models to characterize dynamic behavior of the PU and predict future spectrum holes [5], [6]. Modeling PU activity as a Markov process has been extended to the multiband case For example, optimal per-channel sensing durations for the multiband case were derived in [7].

In the wideband spectrum sensing scenario, an SU must sense an entire band and determine channel boundaries. The bandwidth that must be sensed can vary from the order of 1 MHz to 1 GHz. This is required if the SU can not leverage any external information about channel allocation. A SU need only perform wideband sensing during initialization and may then revert to multiband or narrowband sensing during normal operation. In general, PU signals may be heterogeneous in frequency, bandwidth, and power, so robust wideband sensing algorithms must be developed to detect all PU activity within the spectrum band. State-of-the-art techniques for wideband sensing include wideband energy detection [8] and frequency-domain edge detection [9]. Edge detectors can offer an improvement over energy in terms of SNR threshold, but they can also perform relatively poorly on signals gradual rolloffs in their band edges. Neither technique takes into account the temporal dynamics of PU signals, and consequently can perform rather poorly when PU signals have low duty cycles.

In this paper, we propose a framework for joint time-frequency sensing that outperforms both wideband energy and edge detection techniques particularly in the presence of dynamic PU signals. Moreover, the proposed framework can leverage the large set of existing narrowband sensing techniques. In the proposed sensing algorithm, the spectrum band is is divided into smaller channels and modeled as a balanced binary tree. An HMM is applied to narrowband channel to model the temporal dynamics, and a recursive search for spectrum holes is performed. If any holes are detected that are adjacent in frequency, they are merged into a single spectrum hole, with the objective of maximizing SU capacity over the entire band.

The remainder of the paper is organized as follows. In Section II, we evaluate and compare the performance of

[1]This work was supported in part by the U.S. National Science Foundation under Grants No. 1421869 and No. 1205453.

wideband energy detection and edge detection and demonstrate their limitations in the presence of dynamic PU signals. In Section III, we develop a recursive tree search algorithm to perform joint time-frequency sensing in the wideband regime. In Section IV, we present simulation results that compare the proposed wideband sensing approach to wideband energy detection and edge detection. Concluding remarks are given in Section V.

II. Evaluation of Wideband Energy and Wideband Edge Detection

The wideband energy detector is a very simple wideband sensing technique in which the SU estimates the power spectral density (PSD) over the entire band and applies an energy threshold to determine PU activity [8], [10] . Many PSD frames may be averaged to increase reliability. This simple algorithm has several limitations. Like all energy detectors in additive white Gaussian noise (AWGN), this technique has limited sensitivity, and performance is severely degraded at low SNR. Furthermore, this technique operates on a snapshot in time, and dynamic behavior of the PU will degrade performance, since both the on and off cycles will be averaged into the PSD estimate.

Figs. 1 and 2 depict sensing results of a frequency-domain energy detector for orthogonal frequency division multiplexing (OFDM) and Gaussian minimum shift keying (GMSK) signals, respectively. The simulation experiments were conducted on the GNU radio software platform [11] running on the Ettus N210 USRP board [12]. All of the signals shown have an SNR of 10 dB, but for the dynamic signals, the SNR of the PSD estimate decreases with the duty cycle. This decreased SNR degrades the performance of the energy detector for both modulation schemes.

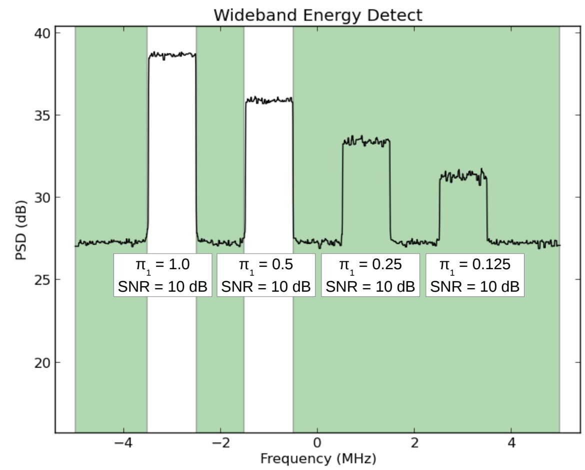

Fig. 1. Results of a wideband energy detector for OFDM signals with 10 dB SNR and 100%, 50%, 25%, and 12.5% duty cycles.

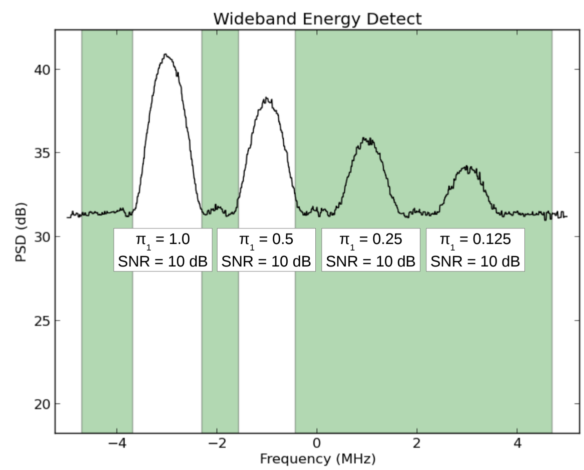

Fig. 2. Results of a wideband energy detector for GMSK signals with 10 dB SNR and 100%, 50%, 25%, and 12.5% duty cycles.

Performing a maximum hold operation rather than averaging PSD frames has been proposed for the detection of dynamic PU signals [13]. However, maximum hold energy detectors are outperformed by averaging detectors in low SNR [13]. Furthermore, maximum hold energy detectors can actually degrade in performance as observation lengths are increased due to increased likelihood of an abnormally high noise power during the sensing duration. These two shortfalls make maximum hold energy detectors inadequate for CR applications and motivate the need for a wideband sensing algorithm that adequately detects dynamic PU activity.

An alternative wideband spectrum sensing technique that has been studied in the literature employs frequency-domain edge detection to determine channel boundaries. A popular edge detection technique uses the continuous wavelet transform to decompose the edge detector into multiple resolutions and multiplies the resolutions together, which has a beneficial effect of reducing the noise [9]. While the edge detectors do offer an improvement over energy detectors in terms of SNR threshold, they come with several limitations. Most importantly, the edge detectors require that PU signals have sharp transitions in the frequency domain. This allows them to work well with the rectangular spectra of OFDM (see Fig. 3) and quadrature amplitude modulation (QAM) with low excess bandwidth, but edge detectors tend to fail on signals with gradual rolloffs on their band edges, such as QAM with large excess bandwidth and GMSK. The performance of an edge detector using the multi-resolution enhancements from [9] is shown for GMSK in Fig. 4.

Furthermore, wideband edge detectors are also degraded by dynamic behavior of the PU. Because energy from idle and active cycles are averaged into the PU detector, the performance of the detector decreases with the duty cycle of the PU. In the next section, we propose a technique that applies narrowband sensing techniques for the wideband scenario. Narrowband techniques that use HMMs to model the dynamic behavior of the PU are leveraged to overcome the limitations discussed for current wideband sensors.

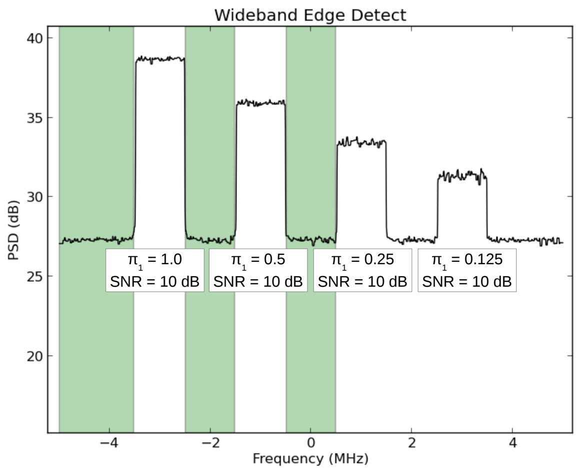

Fig. 3. Results of a wideband edge detector for OFDM signals with 10 dB SNR and 100%, 50%, 25%, and 12.5% duty cycles.

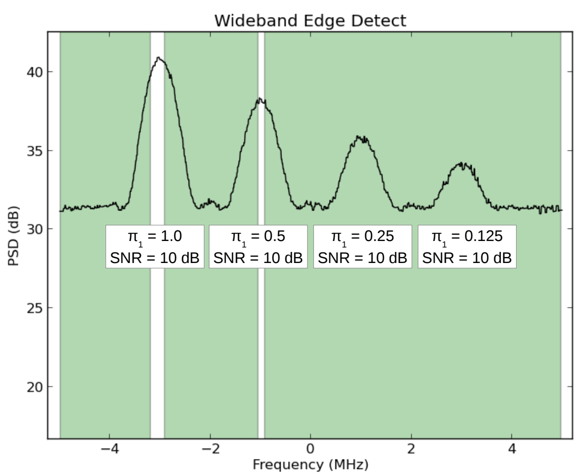

Fig. 4. Results of a wideband edge detector for GMSK signals with 10 dB SNR and 100%, 50%, 25%, and 12.5% duty cycles.

III. Recursive Algorithm for Joint Time-Frequency Sensing

In our proposed algorithm for joint time-frequency sensing, the spectrum band is organized as a balanced binary tree, where each node has two child nodes representing the upper and lower halves of the band. The band is recursively divided into smaller pieces as depth increases [14]. A maximum depth is selected based on a desired resolution for the wideband sensing algorithm. The depth of the tree is defined given by $d_{\text{tree}} = \left\lceil \log_2 \left(\frac{W_0}{W_r} \right) \right\rceil$, where W_0 is the bandwidth, and W_r is the maximum frequency resolution. The division of a band into subbands using a balanced binary tree is shown in Fig 5.

The algorithm recursively divides a given channel in half until the desired resolution is reached. An inorder traversal, a recursive search where child nodes are visited before parent nodes [14] is performed on the balanced binary tree that we use to model the channel. At the highest resolution, the channel is sensed using received signal strength measurements and an HMM is used to model the channel dynamics, assuming a lognormal shadowing model as in [6].

The HMM, denoted by (Y, X), consists of an observable sequence of received signal strengths, $Y = \{Y_k\}_{k=1}^{\infty}$, and a hidden state sequence $X = \{X_k\}$. At time k, Y_k represents the averaged received signal power in logarithmic units (dBm) and X_k represents the state of the PU, i.e., $X_k = 1$ when the PU is idle and $X_k = 2$ when the PU is active. Due to the lognormal shadowing, given $X_k = a$, Y_k is a Gaussian random variable with mean μ_a and variance σ_a^2 for $a = 1, 2$. We shall assume that X is a Markov chain, though it could be extended to a bivariate Markov chain to model non-geometric state sojourn time distributions [6]. Let $G = [g_{ab} : \ a, b \in \{1, 2\}]$ denote the transition matrix of X, where g_{ab} denotes the transition probability from state a to state b. The parameter of the HMM is denoted by $\phi = (G, \boldsymbol{\mu}, \boldsymbol{R})$, where $\boldsymbol{\mu} = [\mu_1, \mu_2]$ and $\boldsymbol{R} = [\sigma_1^2, \sigma_2^2]$. The stationary state probability vector $\boldsymbol{\pi} = [\pi_1, \pi_2]$ can be obtained from G by solving the equations $\boldsymbol{\pi} = \boldsymbol{\pi} G$ and $\pi_1 + \pi_2 = 1$.

The Baum-Welch algorithm [15] is used to obtain a maximium likelihood estimate of the HMM parameter for the given channel. The HMM parameter estimate is then used to calculate an SNR estimate. Let $\mu_{\text{lin},a} = 10^{\frac{\mu_a}{10}}$ denote the mean received signal strength in linear units, i.e., mW, for $a = 1, 2$. Then the SNR estimate is computed as

$$\frac{S}{N} = \frac{\mu_{\text{lin},1} - \mu_{\text{lin},2}}{\mu_{\text{lin},1}}. \tag{1}$$

The capacity of the channel is then estimated using the sensed bandwidth, the estimated SNR, and the stationary distribution of the HMM. The capacity is derived from the capacity for a single user channel with availability π_1 in a TDMA system [16]:

$$C = \pi_1 \log_2 \left(1 + \frac{S}{N} \right). \tag{2}$$

A heuristic test is then performed on the sensing results to determine whether the channel can be used by the SU. The heuristic determines whether the probability that the PU is idle, π_1, surpasses a given threshold $\pi_{\text{min},1}$. If the sensed channel is determined to be usable, the center frequency, bandwidth, and estimated capacity of the channel are passed to the parent node in the tree. As the algorithm recurses upward, the parent nodes combine two lists of channels: one from the lower half of the band, and the other from the upper half of the band. If the highest-frequency channel from the lower band and the lowest-frequency channel from the upper band are adjacent, sensing is then performed on the combination of those two channels and the capacity of the combined channel is estimated. Two channels are combined into a single channel if the following condition is met:

$$C_{a+b} \geq \beta (C_a + C_b), \tag{3}$$

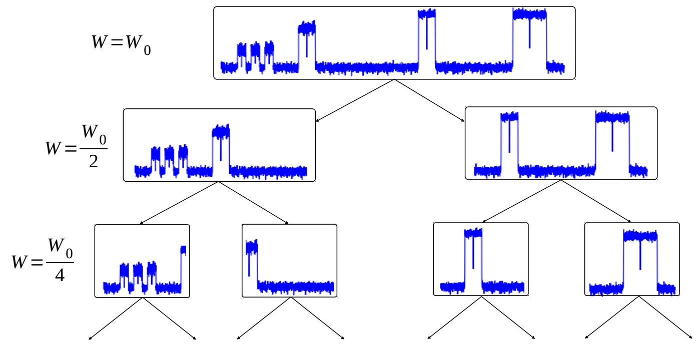

Fig. 5. A spectrum band with center frequency f_{c0} and bandwidth W_0 organized into a balanced binary tree.

TABLE I
ALGORITHM COMPLEXITY PARAMETERS.

Parameter	Description
N_c	Number of channels at the finest sensing resolution
N_t	Number of filter taps for the channel selecting BPF
N_s	Number of samples in the sensing duration
N_i	Number of Baum-Welch iterations
K	Number of HMM states ($K = 2$)

where β is a number between 0 and 1 that represents the inefficiency of splitting a channel into two due to guard bands and other overhead. This test will determine whether using the two channels independently or combining them into a single channel will maximize system throughput for the SU. A more formal description of this wideband sensing framework is given in Algorithm 1.

The computational complexity of the algorithm is given by

$$\mathcal{O}\left(\, (N_c \log_2 N_c) \times \left(N_t N_s + N_i K^2 N_s\right) \, \right), \tag{4}$$

where the various parameters involved are shown in Table I. The terms in the complexity expression 4 are derived as follows: $N_c \log_2 N_c$ is the number of nodes in the binary tree [14] and is therefore the maximum number of narrowband channels that can be sensed; $N_t N_s$ is the complexity of the filtering operation used to select a narrowband channel for sensing. Channel selection may be efficiently performed using a channelizer based on a polyphase decimator, which will efficiently perform the filtering operation and reduce the number of samples tested in the Baum-Welch algorithm [17]. The term $N_i K^2 N_s$ represents the complexity of the Baum-Welch algorithm; N_i may be reduced by choosing initial parameters that represent an educated guess of the PU dynamics [18].

We will not formally describe any of the other functions used in Algorithms 1 and 2, but basic descriptions are given as follows. The function BPF(f_1, f_2) designs a finite impulse response (FIR) bandpass filter between f_1 and f_2. The function FilterAndDecimate($x(n), h(n), \mathrm{dec}$) performs bandpass filtering and decimation on the received wideband signal $x(n)$ using a polyphase channelizer with FIR taps $h(n)$ and decimation rate dec to select the band of

Algorithm 1 Joint time-frequency sensing algorithm.

function RSense(f_c, W, W_r, $x(n)$)
    if $W > W_r$ **then**
        $L_h = \mathrm{RSense}(f_c + W/2, W/2, W_r, X(n))$
        $L_1 = \mathrm{RSense}(f_c - W/2, W/2, W_r, X(n))$
        $L = \mathrm{AggregateCh}(L_h, L_1, X(n))$
    else
        $h(n) = \mathrm{BPF}(f_c - W/2, f_c + W/2)$
        $\mathrm{dec} = \mathrm{Floor}(W_0/W)$
        $y(n) = \mathrm{FilterAndDecimate}(x(n), h(n), drate)$
        $\hat{y}(n) = \mathrm{EnergyTh}(y(n))$
        $(G, \mu, R) = \mathrm{BaumEst}(y(n), \hat{y}(n))$
        if $\pi_1 > \pi_{\min,1}$ **then**
            $C = \mathrm{Capacity}(\boldsymbol{\pi}, \boldsymbol{\mu}, W)$
            return list with single entry (f_c, W, C)

Algorithm 2 Aggregate channels.

function AggregateCh(L_h, L_l, $x(n)$)
    $(f_{c,h}, W_h, C_h) = \mathrm{LowestCh}(L_h)$
    $(f_{c,l}, W_l, C_l) = \mathrm{HighestCh}(L_l)$
    $L = \mathrm{CombineLists}(L_h, L_l)$
    if $f_{c,h} - W_h/2 == f_{c,l} + W_l/2$ **then**
        $h(n) = \mathrm{BPF}(f_{c,l} - W_l/2, f_{c,h} + W_h/2)$
        $\mathrm{dec} = \mathrm{Floor}(W_0/(W_l + W_h))$
        $y(n) = \mathrm{FilterAndDecimate}(x(n), h(n), \mathrm{dec})$
        $\hat{y}(n) = \mathrm{EnergyTh}(y(n))$
        $(G, \mu, R) = \mathrm{BaumEst}(y(n), \hat{y}(n))$
        if $\pi_1 > \pi_{\min,1}$ **then**
            $C = \mathrm{Capacity}(\boldsymbol{\pi}, \boldsymbol{\mu}, W_l + W_h)$
            if $C > \beta(C_h + C_l)$ **then**
                Remove $(f_{c,h}, W_h, C_h)$ and $(f_{c,l}, W_l, C_l)$ from L
                Add $(f_{c,h} + f_{c,k})/2, W_l + W_h, C)$ to L
    return L

interest. The function EnergyTh($y(n)$) performs hard decision energy detection on the selected narrowband channel $y(n)$. The function BaumEst($y(n), \hat{y}(n)$) estimates the parameter of the PU in the selected narrowband channel $y(n)$ using the Baum-Welch algorithm with initial energy detection decisions $\hat{y}(n)$. The function Capacity($\boldsymbol{\pi}, \boldsymbol{\mu}, W$) estimates the channel capacity via (2). The functions HighestCh(L) and LowestCh(L) select the highest-frequency narrowband channel and the lowest-frequency narrowband channel, respectively, from a list of estimated channel parameters L. The function CombineLists(L_1, L_2) merges two lists of estimated channel parameters into a single list and sorts the list in decreasing order of center frequency.

IV. Simulation and Numerical Results

Using the GNU radio/Ettus USRP platform, we tested the wideband energy detector, the wideband edge detector, and the proposed joint time/frequency detector against OFDM and GMSK signals with duty cycles varying among 1.0, 0.5, 0.25, and 0.125. We assumed a minimum duty cycle $\pi_{\text{min},1} = 0.9$ and an overhead per channel of $\beta = 0.3$. For each modulation scheme and duty cycle tested, a wideband capture was generated with signals of random center frequency and baud rate. The modulated data on the signals was generated by a uniform random number generator. All of the signals had an SNR of 10 dB.

Qualitative results are depicted in Fig. 6 for OFDM and Fig. 7 for GMSK. It can be seen that the proposed joint time-frequency detector performed well for all duty cycles and both simulated modulation schemes. The qualitative simulation results of the proposed joint time-frequency detector can be compared to the qualitative results from Section II. Comparing Fig. 6 to Figs. 1 and 3 shows that reducing the duty cycle does not degrade the performance of the proposed detector for OFDM like it does for wideband energy detection. Similarly, a comparison of Fig. 7 to Figs. 2 and 4 shows that the proposed detector is also not degraded by reduced duty cycles for GMSK. Furthermore, comparing Fig. 7 to Fig. 4 shows that the smooth band edges of GMSK do not degrade the performance of the proposed detector like they do for the wideband energy detector.

Quantitative sensing results are depicted by ROC (receiver operating characteristic) curves generated by simulation. Performance of the wideband energy detector is shown in Fig. 8 for OFDM and Fig. 9 for GMSK. The ROC curves were then averaged over many random wideband captures using the same modulation, duty cycle, and SNR. It can clearly be observed that detector performance degrades as PU duty cycle decreases. Performance of the joint time/frequency detector is shown in Fig. 10 for OFDM and Fig. 11 for GMSK. It is clear from these results that the proposed joint time/frequency detector's performance was not significantly degraded by reduced duty cycles.

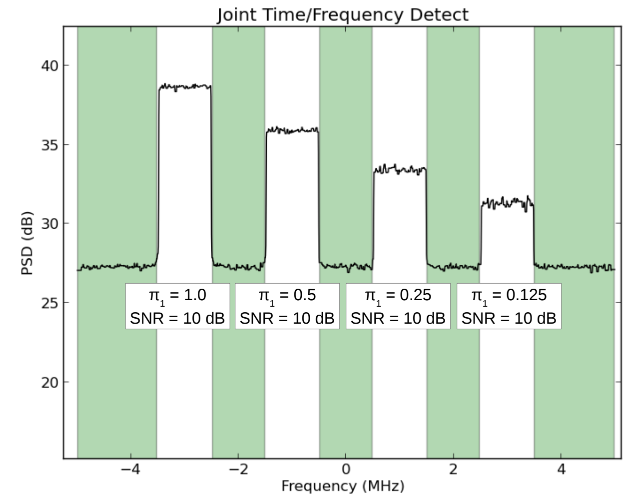

Fig. 6. Results of joint time-frequency detector for OFDM signals with 10 dB SNR and 100%, 50%, 25%, and 12.5% duty cycles.

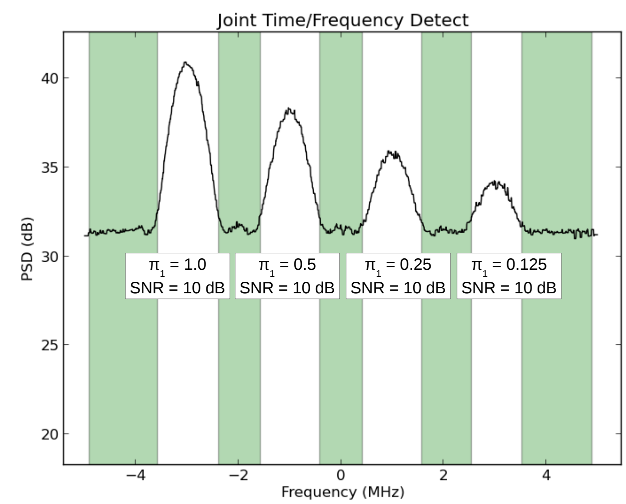

Fig. 7. Results of joint time-frequency detector for GMSK signals with 10 dB SNR and 100%, 50%, 25%, and 12.5% duty cycles.

V. Conclusion

The proposed wideband spectrum sensing framework performs comparably for bursting signals with various duty cycles to to the wideband energy detector applied to signals with 100% duty cycle. For bursting signals, the recursive joint time-frequency sensing algorithm proved to be much more robust than the frequency-only sensing algorithms. The power of the proposed sensing algorithm comes at the cost of computation time; $N_c \log_2 N_c$ narrowband sensing operations must be performed, as well as FIR filtering for channel selection.

We used a simple energy detector as the front-end for the recursive sensing algorithm. Better performance in low SNR could be achieved by applying a state estimation/prediction recursion for an HBMM [6]. Alternative narrowband techniques,

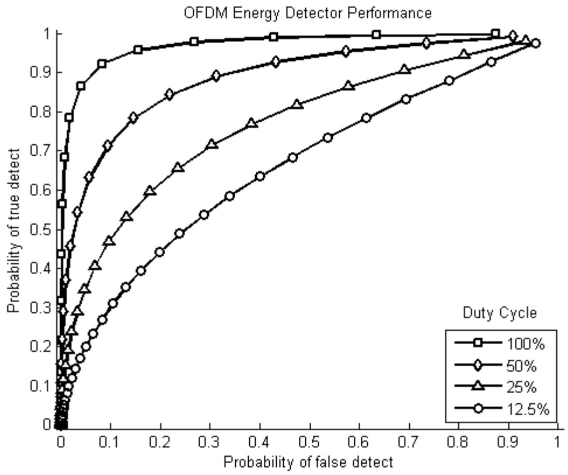

Fig. 8. ROC curve for wideband energy detector for OFDM signals with 10 dB SNR and 100%, 50%, 25%, and 12.5% duty cycles.

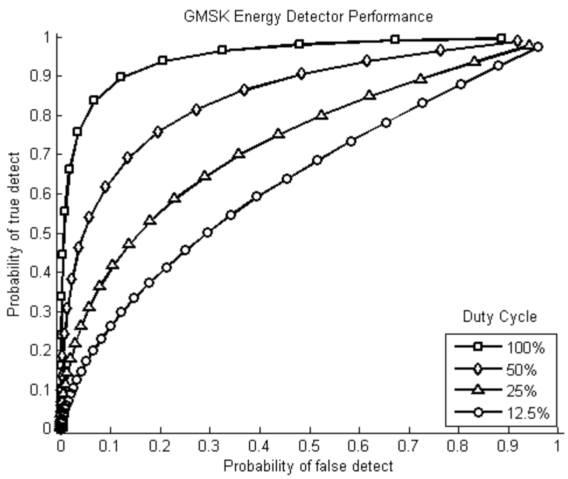

Fig. 9. ROC curve for wideband energy detector for GMSK signals with 10 dB SNR and 100%, 50%, 25%, and 12.5% duty cycles.

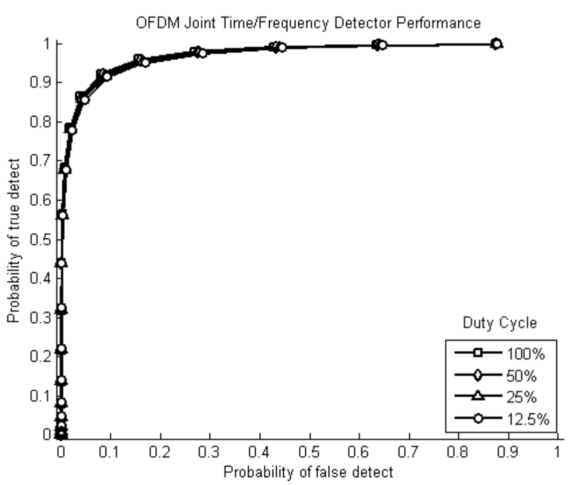

Fig. 10. ROC curve for joint time/frequency detector for OFDM signals with 10 dB SNR and 100%, 50%, 25%, and 12.5% duty cycles.

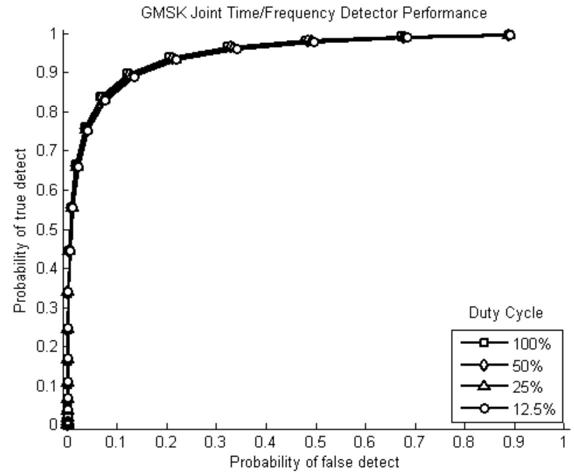

Fig. 11. ROC curve for joint time/frequency detector for GMSK signals with 10 dB SNR and 100%, 50%, 25%, and 12.5% duty cycles.

such as cyclostationary detectors, could also be investigated in conjunction with the proposed wideband sensing framework.

References

[1] FCC, "Spectrum policy task force," Rep. ET Docket, Federal Communications Commission, Tech. Rep. 02-135, Nov. 2002.

[2] S. Haykin, "Cognitive radio: Brain-empowered wireless communications," *IEEE J. Sel. A. Comm.*, vol. 23, no. 2, pp. 201–220, Sep. 2006.

[3] H. Sun, A. Nallanathan, C.-X. Wang, and Y. Chen, "Wideband spectrum sensing for cognitive radio networks: a survey," *Wireless Communications, IEEE*, vol. 20, no. 2, pp. 74–81, April 2013.

[4] T. Yucek and H. Arslan, "A survey of spectrum sensing algorithms for cognitive radio applications," *IEEE Commun. Surveys Tuts.*, vol. 11, no. 1, pp. 116–130, March. 2009.

[5] I. Akbar and W. Tranter, "Dynamic spectrum allocation in cognitive radio using hidden Markov models: Poisson distributed case," in *SoutheastCon, 2007. Proceedings. IEEE*, March 2007, pp. 196–201.

[6] T. Nguyen, B. L. Mark, and Y. Ephraim, "Spectrum sensing using a hidden bivariate Markov model," *IEEE Trans. Wireless Commun.*, vol. 12, no. 9, pp. 4582–4591, Aug. 2013.

[7] P. Tehrani, L. Tong, and Q. Zhao, "Asymptotically efficient multichannel estimation for opportunistic spectrum access," *IEEE Trans. Signal Process.*, vol. 60, no. 10, pp. 5347–5360, Oct. 2012.

[8] D. Cabric, S. Mishra, and R. Brodersen, "Implementation issues in spectrum sensing for cognitive radios," in *Proc. 38th Asilomar Conf. on Signals, Systems and Computers*, vol. 1, Nov. 2004, pp. 772–776.

[9] Z. Tian and G. B. Giannakis, "A wavelet approach to wideband spectrum sensing for cognitive radios," in *Proc. 1st Int. Conf. Cog. Radio Oriented Wireless Nets. and Comms. (CROWNCOM)*, June 2006, pp. 1–5.

[10] M. H. Hayes, *Statistical Digital Signal Processing and Modeling*, 1st ed. New York, NY, USA: John Wiley & Sons, Inc., 1996.

[11] GNU Radio, http://gnuradio.org, accessed: 11-12-2014.

[12] Ettus Research, http://ettus.com, accessed: 11-12-2014.

[13] O. Olabiyi and A. Annamalai, "Extending the capability of energy detector for sensing of heterogeneous wideband spectrum," in *IEEE Consumer Comm. and Net. Conf. (CCNC)*, Jan 2012, pp. 454–458.

[14] D. Knuth, *The Art of Computer Programming, Vol. 1: Fundamental Algorithms*, 3rd ed. Addison-Wesley, 1997.

[15] L. E. Baum and T. Petrie, "Statistical inference for probabilistic functions of finite state Markov chains," *Annals of Mathematical Statistics*, vol. 37, no. 6, pp. 1554–1563, Apr. 1966.

[16] T. M. Cover and J. A. Thomas, *Elements of Information Theory*. Wiley-Interscience, 2006.

[17] F. J. Harris, *Multirate Signal Processing for Communication Systems*. Upper Saddle River, NJ, USA: Prentice Hall PTR, 2004.

[18] Y. Ephraim and N. Merhav, "Hidden Markov processes," *IEEE Trans. Inf. Theory*, vol. 48, no. 6, pp. 1518–1569, June 2002.